Journal of the European Ceramic Society **6** (1990) 161–168

Creep Deformation of Polycrystalline Mullite*

Yasunori Okamoto, Hidetaka Fukudome, Kunio Hayashi & Tomozo Nishikawa

Department of Chemistry and Materials Technology, Kyoto Institute of Technology, Matsugasaki, Sakyo-ku, Kyoto, 606 Japan

(Received 16 October 1989; revised version received 5 March 1990; accepted 19 March 1990)

Abstract

Creep tests for polycrystalline mullites ($3Al_2O_3.2SiO_2$; average grain sizes, $d = 1{\cdot}4$ and $2{\cdot}1\ \mu m$) were carried out in air at temperatures between 1365 and 1480°C. The dependence of steady-state strain rates, $\dot{\varepsilon}$, on stress and grain size was given by $\dot{\varepsilon} \propto \sigma/d^{2.5}$ at lower temperatures ($< 1460°C$) and lower stresses ($< 100\ MPa$), suggesting the deformation mechanism is diffusional creep. Significant cavitation was not observed for deformed specimens. The effective diffusion coefficients were calculated using the rate equation for diffusional creep of mixed oxides, showing very high activation energy ($810\ kJ\ mol^{-1}$). The strain rate apparently increased at higher stresses where fracture often occurred during creep testing within small beam deflections. The SEM examination of fractured specimens revealed two types of fracture mode: slow crack growth pattern observed on the fracture surface of specimens with the small grain size, and cavitation at grain boundaries (intergranular separation) observed on the tensile surface of specimens with the larger grain size.

An polykristallinem Mullit ($3Al_2O_3.2SiO_2$ mit einer durchschnittlichen Korngröße von $1{\cdot}4$–$2{\cdot}1\ \mu m$) wurden zwischen 1365 und 1480°C an Luft Kriechversuche durchgeführt. Die Abhängigkeit der stationären Kriechgeschwindigkeit $\dot{\varepsilon}$ von der Spannung und der Korngröße bei tieferen Temperaturen ($< 1460°C$) und geringeren Spannungen ($< 100\ MPa$) ergab sich zu $\dot{\varepsilon} \propto \sigma/d^{2.5}$ was auf Kriechen durch Diffusion als Verformungsmechanismus schließen läßt. Nennenswerte Porenbildung an Korngrenzen wurde für die verformten Proben nicht beobachtet. Die tatsächlichen Diffusionskoeffizienten wurden aus der Gleichung für Kriechen durch Diffusion gemischter Oxide berechnet und zeigten sehr hohe Aktivierungsenergien ($810\ kJmol^{-1}$). Die Verformungsgeschwindigkeit nahm offensichtlich bei höherer Spannung, wo der Bruch oft während des Kriechversuchs bei kleinen Auslenkungen stattfand, zu. Die rasterelektronenmikroskopische Untersuchung gebrochener Proben zeigte zwei verschiedene Bruchmuster: an der Bruchfläche der Proben mit der kleinen Korngröße wurden Merkmale langsamen Rißwachstums beobachtet, an den Proben mit der größeren Korngröße wurde an der Zugseite der Proben Porenbildung an der Korngrenze (Separation der Körner) beobachtet.

On a effectué des essais de fluage sur des mullites polycristallines ($3Al_2O_3.2SiO_2$; tailles moyennes des grains $d = 1{\cdot}4$ et $2{\cdot}1\ \mu m$) dans l'air à des températures comprises entre 1365 et 1480°C. La vitesse de déformation en régime permanent $\dot{\varepsilon}$ en fonction de la contrainte et de la taille des grains est donnée par la relation $\dot{\varepsilon} \propto \sigma/d^{2.5}$ à basses températures ($< 1460°C$) et pour des contraintes faibles ($< 100\ MPa$), suggérant que le mécanisme de déformation est un fluage diffusionnel. On n'a pas observé de cavitation notable dans les échantillons déformés. Les coefficients de diffusion effectifs ont été calculés à partir de l'équation de vitesse de fluage diffusionnel pour les mélanges d'oxydes, et présentent une énergie d'activation très élevée ($810\ kJ\ mol^{-1}$). La vitesse de déformation croît à l'évidence pour des contraintes élevées où la rupture se produit souvent durant l'essai de fluage à faible allongement de l'éprouvette. L'examen des échantillons révèle deux modes de rupture: propagation lente des fissures observée sur la surface de rupture des échantillons à grains fins et cavitation aux joints de grains (décohésion intergranulaire) sur la surface en traction des éprouvettes à gros grains.

* Presented at the Advanced Materials Science and Engineering Society '89 Conference, Tokyo (Y. Matsuo and M. Sakai: co-chairmen), 16–17 March 1989.

Journal of the European Ceramic Society 0955-2219/90/$3.50

1 Introduction

Dense polycrystalline mullites with a little or no glassy phases have become available by sintering fine mullite powders,[1-3] and the mechanical properties, including the creep behavior, of those ceramics have been reported.[3-8] Although mullite polycrystals were shown to have excellent creep resistance at high temperatures, the deformation mechanisms are not completely clarified because of insufficient data on the creep behavior (the dependence of creep rate on grain size, stress and temperature) and on the diffusivity of ions in mullite. The deformation of polycrystalline silicates such as mullite and forsterite (olivine), itself, is of interest.

In the present study, bending creep tests were carried out to elucidate the deformation mechanisms. Some data on creep fracture were also obtained during the course of experiments.

2 Experimental

The polycrystalline mullite samples were obtained by sintering a fine powder prepared using the sol–gel method by Chichibu Cement Co., Tokyo, Japan, of nominally stoichiometric mullite ($3Al_2O_3 . 2Si_2O_3$) at 1650°C for 2 h (sample A). (The major impurities are TiO_2 <0·2 wt%, Fe_2O_3 <0·01 wt%, Na_2O and K_2O <0·01. The lattice parameters determined by the XRD measurements are: $a = 7{\cdot}5466$, $b = 7{\cdot}6932$ and $c = 2{\cdot}8847$ Å. The samples were sintered by Hitachi Zosen, Corp., Osaka, Japan.) A few of these samples were subsequently annealed at 1680°C for 10 h to obtain coarser grained samples (sample B). The average grain sizes of samples A and B were 1·4 and 2·1 μm, respectively (the average linear intercepts multiplied by the factor of 1·5). The specimens with average dimensions of 2 × 4·5 × 45 mm were machined, polished, and then chamfered.

Creep tests were carried out in air in four-point bending using fixtures made of dense, coarse-grained alumina, at temperatures between 1365 and 1480°C, and at stresses ranging from 10 to 100 MPa. The major and minor spans were 35 and 11 mm, respectively. After an apparent steady state occurred at an applied load, the load was increased (incremental stress testing). For a bend bar with rectangular cross-section of width w and height h, the outer-fiber stress, σ, and the outer-fiber strain rate, $\dot{\varepsilon}$, were calculated using the equations derived by Hollenberg *et al.*:[9]

$$\sigma = \frac{3(L-l)P}{2wh^2}\left(\frac{2n+1}{3n}\right) \tag{1}$$

$$\dot{\varepsilon} = \frac{2h(n+2)\dot{x}}{(L-l)[L+l(n+1)]} \tag{2}$$

Here, P is the load, n is the stress exponent, $\dot{x}$ is the load point displacement rate, L and l are the major and minor spans, respectively. The calculation was limited to the maximum outer-fiber strain of ≈3%.

The tensile surfaces and creep-fracture surfaces were examined in a scanning electron microscope (SEM) with attention to grain growth, creep damage (cavitation) and fracture mode.

3 Results

Figure 1 shows the microstructures of as-received samples. Some pores are present at grain boundaries. Apparent glassy phases are not observed. However, traces of a glassy phase at the grain boundaries were reported for a mullite which was sintered using the

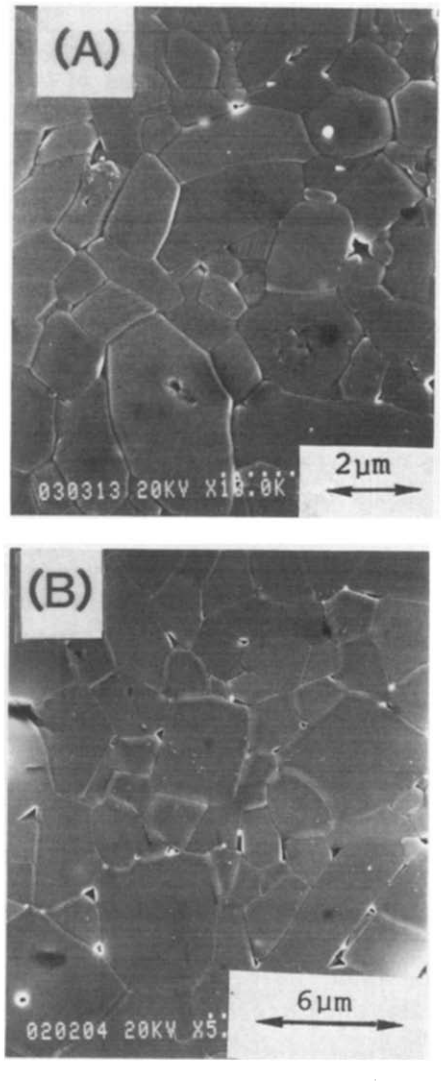

Fig. 1. Microstructures of mullite samples A and B, thermally etched after polishing.

Table 1. Some mechanical properties of sample A

Density (% theoretical)	>98
Young's modulus, E (GPa)[a]	224
Flexural strength, σ_f (MPa)	301 ± 17
Vickers hardness, H_v (GPa)	10·2 ± 0·4
Fracture toughness, K_{IC} (MPam$^{1/2}$)[b]	2·7 ± 0·1

[a] Flexural resonance technique.
[b] Indentation fracture method. $K_{IC} = 0{\cdot}036E^{0{\cdot}4}P_i^{0{\cdot}6}a^{-0{\cdot}7}(c/a)^{-1{\cdot}5}$, where P_i is the indentation load, a is the impression radius and c is the radial crack length.[10]

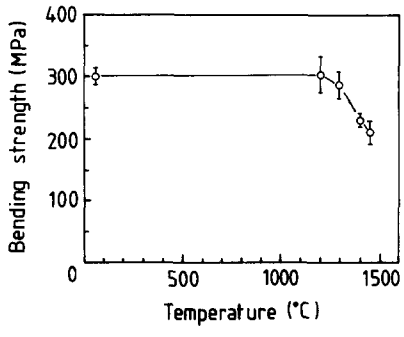

Fig. 2. Flexural strength as a function of temperature for sample A, tested in three-point bending (span = 30 mm).

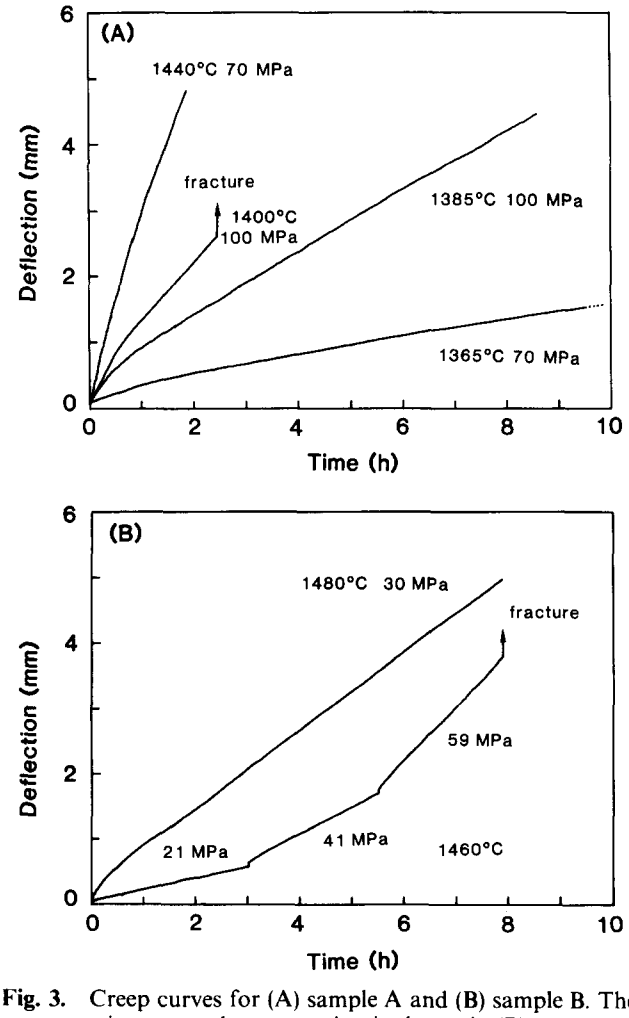

Fig. 3. Creep curves for (A) sample A and (B) sample B. The incremental stress testing is shown in (B).

same powder.[7] Some mechanical properties of sample A are given in Table 1. Figure 2 shows the flexural strength as a function of temperature (sample A).

Figure 3 shows some typical creep curves for samples A and B. After a transient creep for 1 to 2 h, an apparent steady state was established. The tertiary creep was not observed at the stress where creep fracture occurred. The plots of steady-state strain (creep) rates, $\dot{\varepsilon}$, versus stress, σ, are shown in Fig. 4. The stress exponent, n, was ≈ 1 at lower temperatures and lower stresses (i.e. Newtonian behavior), while it increased at higher temperatures (1480°C and 1460°C at higher stresses for sample A). It is also noted that the strain rates increased at higher stresses just lower than those at which creep fracture occurred, resulting in the increase in the value of n. Figure 5 shows the dependence of strain

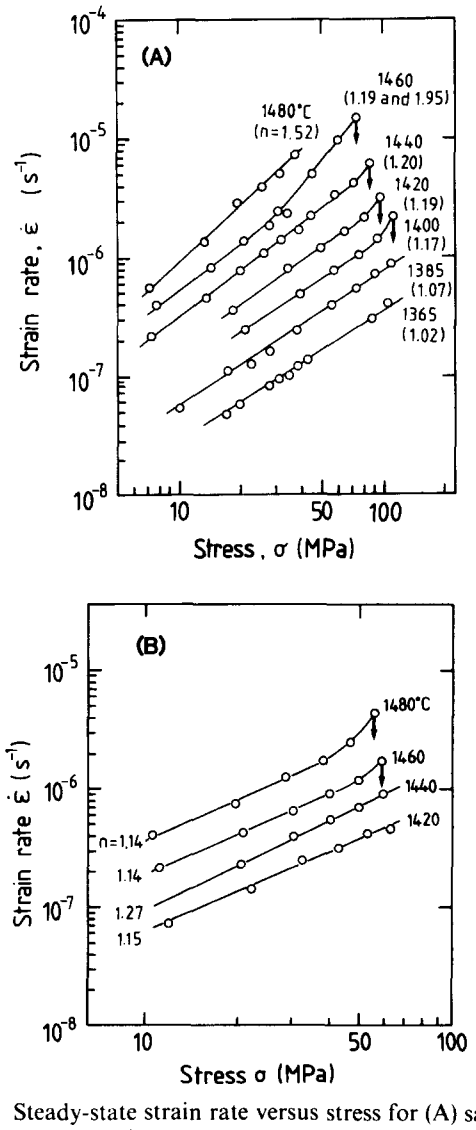

Fig. 4. Steady-state strain rate versus stress for (A) sample A and (B) sample B. The arrows indicate the stresses at which the specimens fractured during creep testing within apparent outer-fibre strain ≤ 3%.

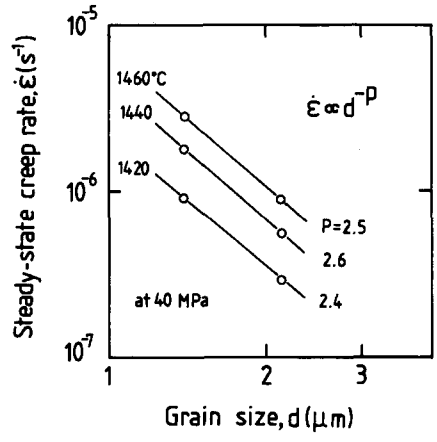

Fig. 5. Effect of grain size on strain rate for creep of mullite in the Newtonian region ($n \approx 1$).

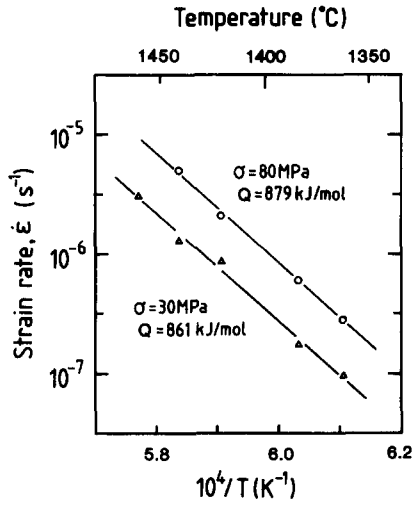

Fig. 6. Temperature dependence of strain rate for mullite (sample A).

rate on grain size, d, at a stress of 40 MPa (Newtonian region), indicating $p \approx 2{\cdot}5$, where p is the grain size exponent defined by $\dot{\varepsilon} \propto \sigma^n/d^p$. The temperature dependence of strain rate is shown in Fig. 6, indicating a relatively high activation energy for creep deformation ($\approx 870\,\mathrm{kJ\,mol^{-1}}$). The specimens which have deformed in the Newtonian region show no evidence of cavitation on the tensile surface. No grain growth during creep testing occurred in both samples.

4 Discussion

The results shown in Figs 4 and 5 suggest that the deformation of both mullite samples is diffusional creep in a large portion of the stress–temperature field tested. In the diffusional creep of mullite ($Al_6Si_2O_{13}$), the strain rate is given by[11,12]

$$\dot{\varepsilon} = \frac{14\sigma\Omega_M}{d^2kT} D_{eff} \qquad (3)$$

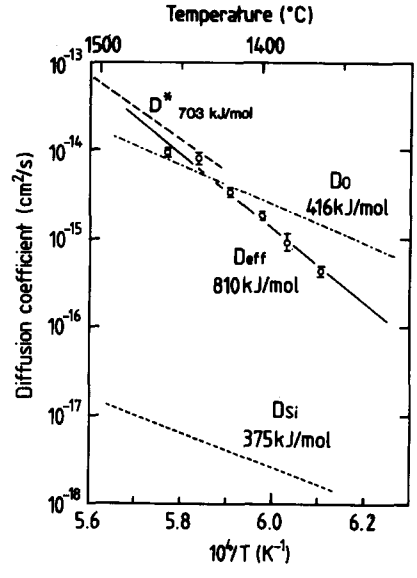

Fig. 7. Effective diffusion coefficients (D_{eff}) calculated from creep strain rates using eqn (3) for diffusional creep region ($n \approx 1$). D_O and D_{Si} are diffusion coefficients of O[14,16] and Si[14,17] respectively, in forsterite. D^* is diffusion coefficients in mullite.[15] Activation energies are specified on the figure.

where Ω_M is the 'molecular' volume ($=2{\cdot}23 \times 10^{-22}\,cm^3$ for stoichiometric mullite), k is Boltzmann's constant, T is the temperature and D_{eff} is the effective diffusion coefficient for the 'molecule' $Al_6Si_2O_{13}$:

$$D_{eff} = \frac{1}{(6/D^e_{Al}) + (2/D^e_{Si}) + (13/D^e_O)} \qquad (4)$$

where D^e_A is the effective diffusion coefficient of ion A (A = Al, Si and O):

$$D^e_A = D^l_A + (\pi/d)\delta D^b_A \qquad (5)$$

where D^l_A is the lattice diffusion coefficient of A, D^b_A is the boundary diffusion coefficient of A and δ is the grain-boundary width. Considering the structure of mullite, which has a number of oxygen vacancies in the lattice,[13] and taking account of the analogy to the structure of forsterite (Mg_2SiO_4),[14] it is inferred that $D^l_{Al} > D^l_O > D^l_{Si}$. At present, however, there is little information on the diffusion coefficients of ions in mullite, with an exception of the data reported by Aksay *et al.*[15] The grain-size exponent p ($=2{\cdot}5$) shown in Fig. 5 suggests that the diffusion of the rate-limiting species both through the lattice and along the grain boundaries controls the deformation (eqn (5)); i.e. both Nabarro–Herring creep and Coble creep contribute to the overall strain rate. Effective diffusion coefficients calculated in the diffusional creep region ($n \approx 1$) using eqn (3) are plotted in Fig. 7, where the least-squares line (solid line) is given by

$$D_{eff} = 3{\cdot}6 \times 10^{10} \exp(-810 \pm 13\,[\mathrm{kJmol^{-1}}]/RT) \quad [\mathrm{cm^2\,s^{-1}}]$$

Table 2. Stress exponents (n) and activation energies (Q) for creep deformation of mullite

Testing	*Temperature* (°C)	*n*	*Q* ($kJ\,mol^{-1}$)	*Reference*
Hot pressing	1 450–1 650	1·4	707	18
Bending	1 350–1 450	1·0	687	4
Compression	1 400–1 500	1·0	710	5
Tension	1 350–1 450	1·6	900	19
Bending	1 400–1 500	1·3	—	20
Bending	1 400–1 500	1·4	703	21
Compression	1 400–1 550	1·3	1 030	22
Bending	1 365–1 480	1·0	810[a]	Present study

[a] Q in D_{eff}.

Diffusivities in mullite[15] and those of Si and O in forsterite[14,16,17] are also plotted for comparison. Note that the activation energy in mullite is very high compared to those for Si and O in forsterite. The apparent activation energies and stress exponents for the deformation of mullite so far reported are listed in Table 2. The high value of activation energy in the present work as well as those reported by Kumazawa *et al.*[19] and Ohira *et al.*[22] is remarkable. These high activation energies are unlikely to be due to the contribution of grain-boundary diffusion to the deformation. Davis & Pask[23] have shown that the diffusion through a liquid of the Al_2O_3–SiO_2 system depends on the concentration of Al_2O_3 and shows higher apparent activation energies at lower Al_2O_3 contents (e.g., $\approx 1300\,kJmol^{-1}$ at 4 wt% Al_2O_3). Furthermore, polycrystals containing glassy phases at grain boundaries deform via pressure solution (solution precipitation), showing high apparent activation energies.[24–26] However, the stress exponents obtained at higher temperatures are higher than 1 (Fig. 4(A)), which implies dislocation creep ($n \geq 3$) or interface-reaction controlled deformation ($n = 2$) rather than solution precipitation ($n = 1$). Further testing, especially at higher temperatures, as well as the investigation of diffusion of ions through lattice and along grain boundaries in mullite are necessary.

Any cavity formation was not observed on the tensile surface of deformed and creep-fractured specimens of sample A (Fig. 8). A little cavitation, seen in Fig. 8(A), which shows the tensile surface of a specimen (deformed with $n \approx 2$), is not responsible for creep strain. On the fracture surface of sample A, a slow crack growth (SCG) pattern was observed (Fig. 9). Intergranular fracture is predominant in the semi-elliptical SCG region, while transgranular fracture is predominant in the outside of the region, showing catastrophic fracture. The apparent increase in strain rate at the fracture stresses (at temperatures between 1400 and 1440°C in Fig. 4(A)) may be induced by slow crack growth. Supposing the SCG region is the origin of catastrophic fracture, though the samples are deformed, the fracture toughness was calculated approximately using the dimensions of the SCG pattern (the controlled surface flaw technique[27]), resulting in an average value of $3{\cdot}5\,MPa\,m^{1/2}$ at 1420°C. Apparent fracture toughness appeared to increase at these high temperatures, in spite of the decrease in strength (see Table 1 and Fig. 1). Fast fracture in three-point bending (Fig. 2; elastic strain rate $\approx 1{\cdot}7 \times 10^{-4}\,s^{-1}$) was completely transgranular at these temperatures. Sample A has higher strength and higher toughness than those of the hot-pressed, translucent mullite investigated by Mah & Mazdiyasni.[6]

On the other hand, the creep fracture of sample B was completely intergranular, as seen in Fig. 9. In addition, many cavities (intergranular separation) were observed on the tensile surface of fractured specimens (Fig. 8(B)), though significant cavitation was not observed for the specimens deformed at lower stresses without fracture. The cavity nucleation and growth appeared to occur at the fracture stress without any apparent tertiary creep. These results suggest that the mechanism of creep fracture in sample B is different from that in sample A; i.e. slow crack growth from a fracture origin in sample A, and cavity growth at isolated origins and their coalescence in sample B. Thus, for sample B, the apparent increase in strain rate at stresses near the stress where creep fracture occurred, as seen in Fig. 4(B), seems to be due to cavity growth.

Stress and strain (rate) are not correctly evaluated using eqns (1) and (2) in the regions where the deformation is accompanied by creep damages.[28,29] However, Newtonian flow without any significant cavitation was predominant at the temperatures and stresses tested, where the estimation of stress and strain rate was believed to be appropriate, although the investigation of deformation behavior in tension or compression may be desirable. Additional studies of the effect of glassy phases at grain boundaries, if any, on deformation and fracture are also required for further discussion.

5 Conclusions

(1) In creep deformation of dense, single-phase, stoichiometric mullite polycrystals ($d = 1{\cdot}4$ and $2{\cdot}1\,\mu m$), the dependence of steady-state strain rate on stress and grain size ($\dot{\varepsilon} \propto \sigma/d^{2{\cdot}5}$) suggests that diffusional creep dominates at

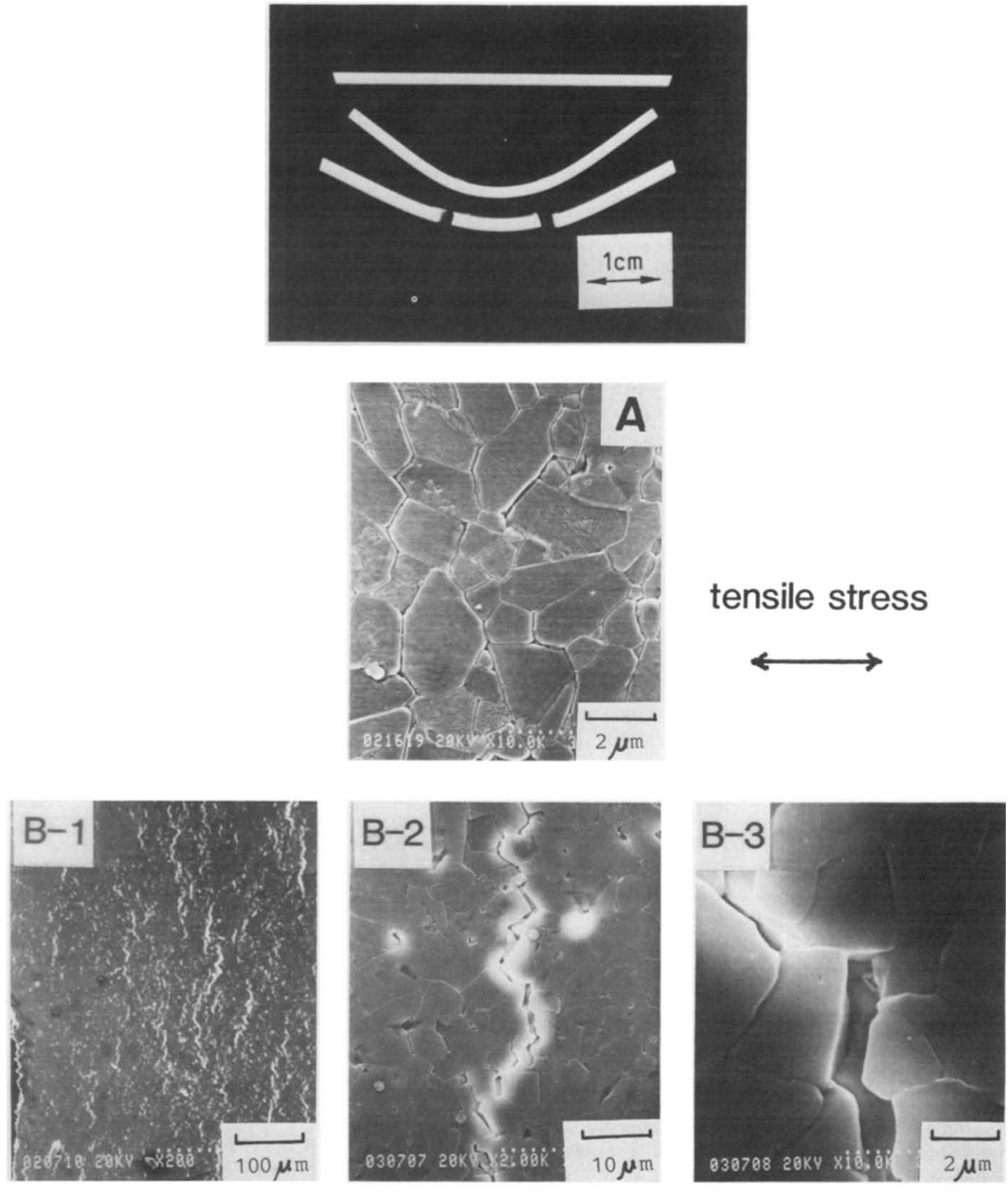

Fig. 8. Deformed and fractured samples and scanning electron micrographs of tensile surfaces of creep-fractured mullite for (A) sample A tested at 1460°C, 86 MPa; $\varepsilon = 2{\cdot}8\%$, and (B) sample B tested at 1480°C, 56 MPa; $\varepsilon = 3{\cdot}9\%$. Significant cavitation is observed on the tensile surface of sample B (B-1 to B-3).

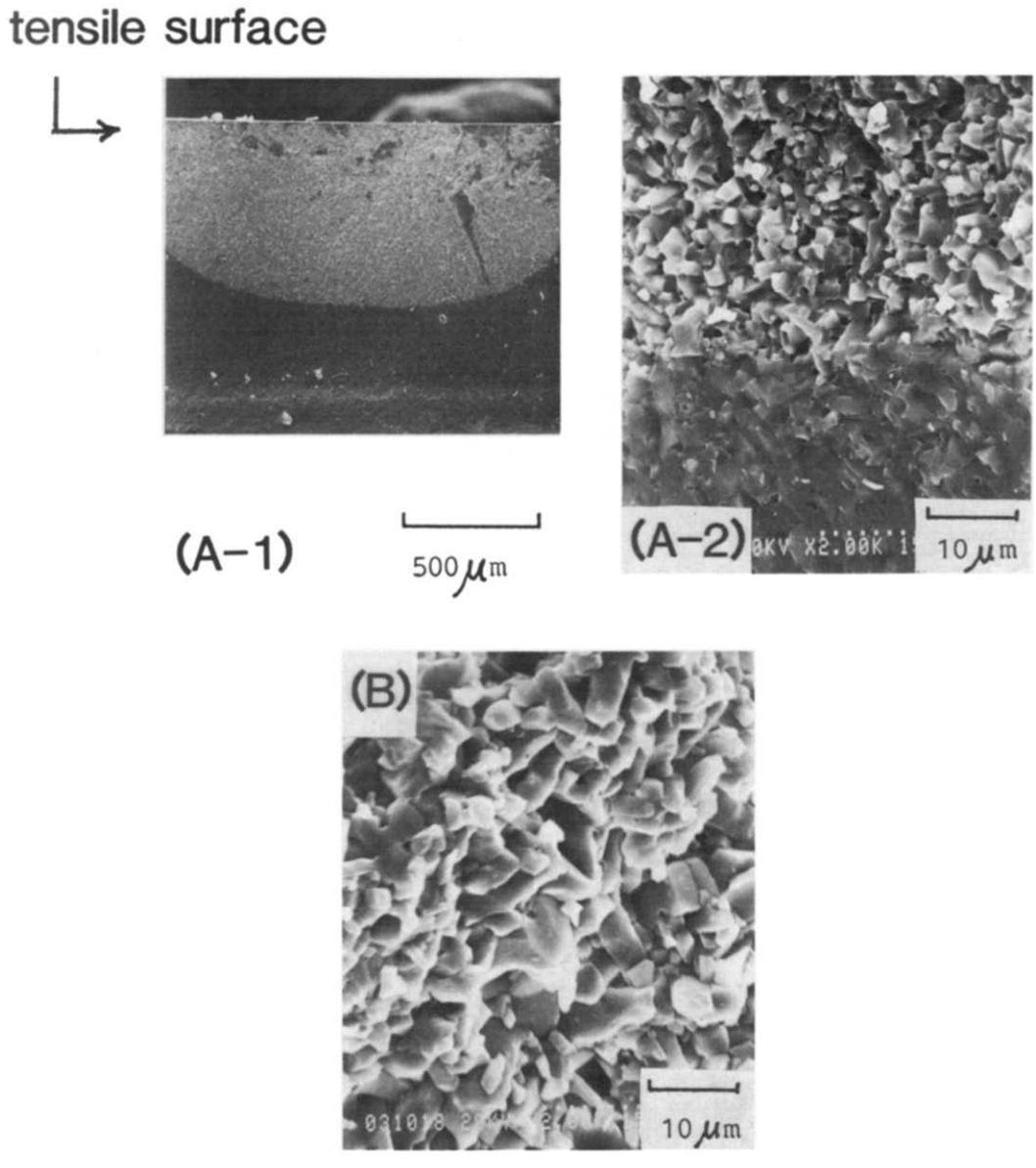

Fig. 9. Scanning electron micrographs of fracture surfaces. (A-1) Sample A tested at 1400°C and 113 MPa ($\varepsilon = 2{\cdot}6\%$), showing slow crack growth; (A-2) boundary region between SCG fracture and catastrophic, transgranular fracture; (B) sample B tested at 1480°C and 56 MPa ($\varepsilon = 3{\cdot}9\%$), showing intergranular fracture on the whole fracture surface.

lower temperatures (< 1460°C) and at lower stresses (< 100 MPa). Significant cavitation was not observed for deformed specimens.

(2) Effective diffusion coefficients calculated in the temperature range from 1360 to 1460°C are expressed as:

$$D_{\text{eff}} = 3{\cdot}6 \times 10^{10} \exp\left(\frac{-810 \pm 13[\text{kJmol}^{-1}]}{RT}\right) \times [\text{cm}^2\,\text{s}^{-1}]$$

(3) The increase in strain rate observed at higher stresses are due to slow crack growth (especially for sample A) or intergranular cavitation (especially for sample B).

Acknowledgement

The authors thank J. Yano, Hitachi Zosen, Corp., for providing the mullite samples.

References

1. Mazdiyasni, K. S. & Brown, L. M., Synthesis and mechanical properties of stoichiometric aluminum silicate (mullite). *J. Amer. Ceram. Soc.*, **55**(11) (1972) 548–52.
2. Ghate, B. B., Hasselman, D. P. H. & Spriggs, R. M., Synthesis and characterization of high purity, fine grained mullite. *Amer. Ceram. Soc. Bull.*, **52**(9) (1973) 670–2.
3. Kanzaki, S., Tabata, H., Kumazawa, T. & Ohta, S., Sintering and mechanical properties of stoichiometric mullite. *J. Amer. Ceram. Soc.*, **65**(1) (1985) C-6–C-7.

4. Lessing, P. A., Gordon, R. S. & Mazdiyasni, K. S., Creep of polycrystalline mullite. *J. Amer. Ceram. Soc.*, **58**(3–4) (1975) 149.
5. Dokko, P. C., Pask, J. A. & Mazdiyasni, K. S., High-temperature mechanical properties of mullite under compression. *J. Amer. Ceram. Soc.*, **60**(3–4) (1977) 150–5.
6. Mah, T.-I. & Mazdiyasni, K. S., Mechanical properties of mullite. *J. Amer. Ceram. Soc.*, **66**(10) (1983) 699–703.
7. Ismail, M. G. M. U., Nakai, Z. & Sōmiya, S., Microstructure and mechanical properties of mullite prepared by the sol–gel method. *J. Amer. Ceram. Soc.*, **70**(1) (1987) C-7–C-8.
8. Kumazawa, T., Kanzaki, S., Ohta, S. & Tabata, H., Influence of chemical composition on mechanical properties of SiO_2–Al_2O_3 ceramics. *Nippon Seramikkusu Kyokai Gakujutsu Ronbunshi* (*J. Ceram. Soc. Jpn*), **96**(1) (1988) 85–91.
9. Hollenberg, G. W., Terwilliger, G. R. & Gordon, R. S., Calculation of stresses and strains in four-point bending creep tests. *J. Amer. Ceram. Soc.*, **54**(4) (1971) 196–9.
10. Marshall, D. B. & Evans, A. G., Reply to Comment on "Elastic/plastic indentation damage in ceramics: The median/radial crack system"'. *J. Amer. Ceram. Soc.*, **64**(12) (1981) C-182–C-183.
11. Gordon, R. S., Ambipolar diffusion and its application to diffusion creep. In *Mass Transport Phenomena in Ceramics* (*Materials Science Research, Vol. 9*), ed. A. R. Cooper & A. H. Heuer. Plenum Press, New York, 1975, pp. 445–64.
12. Cannon, R. M. & Coble, R. L., Review of diffusional creep of Al_2O_3. In *Deformation of Ceramic Materials*, ed. R. C. Bradt & R. E. Tressler. Plenum Press, New York, 1975, pp. 61–99.
13. Cameron, W. E., Mullite: A substituted alumina. *Amer. Mineral.*, **62** (1977) 747–55.
14. Kohlstedt, D. L. & Ricoult, D. L., High-temperature creep of silicate olivines. In *Deformation of Ceramic Materials II* (*Materials Science Research, Vol. 18*), ed. R. E. Tressler & R. C. Bradt. Plenum Press, New York, 1984, pp. 251–80.
15. Aksay, I. A., Davis, R. F. & Pask, J. A., Diffusion in mullite (abstract). *Amer. Ceram. Soc. Bull.*, **52**(9) (1973) 710.
16. Ando, K., Kurokawa, H., Oishi, Y. & Takei, H., Self-diffusion coefficient of oxygen in single-crystal forsterite. *J. Amer. Ceram. Soc.*, **64**(2) (1981) C-30.
17. Jaoul, O., Poumellec, M., Froidevaux, C. & Havette, A., Silicon diffusion in forsterite. In *Anelasticity in the Earth*, ed. F. D. Stacey, M. S. Paterson & A. Nicolas. Amer. Geophys. Union and Geol. Soc. Amer., Washington and Boulder, 1981, pp. 95–100.
18. Penty, R. A., Hasselman, D. P. H. & Spriggs, R. M., Pressure sintering kinetics of fine-grained mullite by the change in pressure and temperature technique. *Amer. Ceram. Soc. Bull.*, **52**(9) (1973) 692–3.
19. Kumazawa, T., Kanzaki, S., Wakai, F. & Tabata, H., Creep behaviour of mullite ceramics. In *Proceedings of Basic Science Divisional Meeting of the Ceramic Society of Japan*, Ceramic Society of Japan, 1987, p. 206.
20. Tomatsu, H., Maeda, K., Ohnishi, H. & Kawanami, T., High temperature creep of mullite ceramics. In *Proceedings of Annual Meeting of the Ceramic Society of Japan*, Ceramic Society of Japan, 1987, pp. 51–2.
21. Ashizuka, M., Okuno, T. & Kubota, Y., Creep of mullite ceramics. In *Proceedings of Annual Meeting of the Ceramic Society of Japan*, Ceramic Society of Japan, 1987, p. 173, also published as: Creep of mullite ceramics. *Nippon Seramikkusu Kyokai Gakujutsu Ronbunshi* (*J. Ceram. Soc. Jpn*), **97**(6) (1989) 662–8.
22. Ohira, H., Shiga, H., Ismail, M. G. M. U., Nakai, Z., Akiba, T. & Yasuda, E., Compressive creep behavior of mullite ceramics. In *Proceedings of Annual Meeting of the Ceramic Society of Japan*, Ceramic Society of Japan, 1989, p. 12.
23. Davis, R. F. & Pask, J. A., Diffusion and reaction studies in the system Al_2O_3–SiO_2. *J. Amer. Ceram. Soc.*, **55**(10) (1972) 525–31.
24. Wan, J.-G. & Raj, R., Mechanism of superplastic flow in a fine-grained ceramic containing some liquid phase. *J. Amer. Ceram. Soc.*, **67**(6) (1984) 399–409.
25. Wiederhorn, S. M., Hockey, B. J., Krause, Jr, R. F. & Jakus, K., Creep and fracture of a vitreous-bonded aluminium oxide. *J. Mater. Sci.*, **21** (1986) 810–24.
26. Okamoto, Y., Nishi, T., Nishida, T., Hayashi, K. & Nishikawa, T., Creep and creep cavitation in polycrystalline MgO: Effect of intergranular second phase. In *Sintering '87: Proceedings of the 4th International Symposium on Science and Technology of Sintering*, Tokyo, ed. S. Sōmiya, M. Shimada, M. Yoshimura & R. Watanabe. Elsevier Applied Science, London, New York, Tokyo, 1988, pp. 825–30.
27. Petrovic, J. J., Jacobson, L. A., Talty, P. K. & Vesudevan, A. K., Controlled surface flaws in hot-pressed Si_3N_4. *J. Amer. Ceram. Soc.*, **58**(3–4) (1975) 113–16.
28. Chuang, T.-J., Estimation of power-law creep parameters from bend test data. *J. Mater. Sci.*, **21** (1986) 165–75.
29. Chuang, T.-J. & Wiederhorn, S. M., Damage-enhanced creep in a siliconized silicon carbide: Mechanics of deformation. *J. Amer. Ceram. Soc.*, **71**(7) (1988) 595–601.